Fire Safety Journal 61 (2013) 243–253

Contents lists available at ScienceDirect

Fire Safety Journal

journal homepage: www.elsevier.com/locate/firesaf

Fire behaviors of polymers under autoignition conditions in a cone calorimeter

Long Shi *, Michael Yit Lin Chew

Department of Building, National University of Singapore, Singapore 117566, Singapore

ARTICLE INFO

Article history:
Received 24 August 2012
Received in revised form
3 June 2013
Accepted 3 September 2013

Keywords:
Spontaneous ignition
Non-charring polymer
Heat release rate
Mass loss rate
Thermal thickness
Cone calorimeter

ABSTRACT

Besides piloted ignition, autoignition is also an important aspect to real fire development as combustible materials may be ignited without independent flame. Fire behaviors of non-charring and charring polymers were then investigated in a cone calorimeter under autoignition conditions. Fire risk of non-charring polymers are higher than those of charring polymers because of high heat release, and the increase of heat release rate is much obvious with a higher heat flux or thickness. Charring polymers seem to have a higher CO yield, while non-charring polymers have a higher CO_2 yield. Ignition methods have influences to combustion efficiency of non-charring polymers as effective heat of combustion under autoignition are observed lower than those reference data under piloted ignition conditions. Its influences to charring polymers are not obvious. Both CO and CO_2 yields under flaming combustion are higher than those under non-flaming combustion, but mass percent of carbon seem to has limited effect. Experimental data in this study can provide a guidance to fire risk evaluation of non-charring and charring polymers.

1. Introduction

Ignition may be defined as that process by which a rapid, exothermic reaction is initiated, which then propagates and causes material involved to undergo change, producing temperature greatly in excess of ambient [1]. There are two types of ignition, namely piloted ignition – in which flaming is initiated in a flammable vapour/air mixture by a 'pilot', such as an electrical spark or an independent flame – and autoignition (or spontaneous ignition)—in which flaming develops spontaneously within the mixture [1]. Piloted ignition of a solid might very roughly be considered as occurring when lower flammability limit of a pyrolysate/air mixture is first reached, while autoignition of a solid might be considered to involve the autoignition of pyrolysates [2]. Besides piloted ignition, autoignition process is also an important aspect to describe real fire development as combustible materials may be ignited without acceleration of spark plug or independent flame under specific situations. Combustible materials have been well investigated under piloted ignition [3–11], however, few studies have focused on fire behaviors under autoignition conditions.

Combustible materials showed different fire behaviors under piloted ignition and autoignition conditions. From statistical analysis of experimental results, Melinek [12] noticed that minimum rate of volatile emission can be used to predict ignition, which is about 5.1 g/m^2 s for piloted ignition and 7.7 g/m^2 s for autoignition. Different empirical models on ignition time were obtained for woods under piloted ignition [2,13] and autoignition [14,15] conditions. A correlation of ignition time for woods under piloted ignition and autoignition was obtained by Babrauskas [13]. It was shown that autoignition time are longer than piloted ignition time, and difference between these two becomes smaller as external heat flux rises. Minimum heat flux under autoignition also were found to be much higher than those under piloted ignition [2]. Cain [16] obtained that average minimum heat flux under autoignition are about 2.37 times of those under piloted ignition.

External heat flux was found to impact fire behaviors of combustible materials. Shi and Chew [17] investigated fire behaviors of woods under autoignition in a cone calorimeter. Experimental results showed that CO yield are less than 0.025 g/g when external heat flux are higher than 50 kW/m^2, but they become higher than 0.04 g/g under 25 kW/m^2 heat flux. Luche et al. [4] investigated influences of external heat flux to fire behaviors of black PMMA in a cone calorimeter. It was observed that average *MLR* increases linearly with external heat flux.

Gas production show differences when materials are under non-flaming and flaming combustions. Non-flaming combustion (also called pyrolysis) is used to refer to a stage of fire before flaming combustion has occurred [2]. Flaming combustion is defined as an exothermic oxidation reaction that takes place in

* Corresponding author. Tel.: +65 83818700.
E-mail addresses: shilong@mail.ustc.edu.cn, shilong@nus.edu.sg (L. Shi).

0379-7112/$ - see front matter © 2013 Published by Elsevier Ltd.
http://dx.doi.org/10.1016/j.firesaf.2013.09.021

Nomenclature

C_P	specific heat capacity (J/kg/K)
[C]	mass percent of carbon (%)
EHC	effective heat of combustion (kJ/g)
HRR	heat release rate (kW/m^2)
$\overline{HRR}$	average heat release rate (kW/m^2)
MLR	mass loss rate (g/s/m^2)
$\overline{MLR}$	average mass loss rate (g/s/m^2)
$\dot{q}''$	external heat flux (kW/m^2)
t_{ig}	ignition time (s)
y	gas yield (g/g)
y'	gas yield under non-flaming condition (g/g)
y''	gas yield under flaming condition (g/g)

Greek letters

δ_P	thermal thickness (mm)
λ	thermal conductivity (W/m/K)
ρ	density (kg/m^3)

Subscripts

25	values under 25 kW/m^2 heat flux
50	values under 50 kW/m^2 heat flux
75	values under 75 kW/m^2 heat flux
CO	carbon monoxide
CO_2	carbon dioxide

Abbreviations

ABS	acrylonitrile butadiene styrene
CO	carbon monoxide
CO_2	carbon dioxide
HDPE	high-density polyethylene
HIPS	high impact polystyrene
PC	Polycarbonate
PET	polyethylene terephthalate
PMMA	polymethyl methacrylate
PP	polypropylene
PVC	polyvinyl chloride

the gas phase, resulting in high temperature gases which would be visible to the naked eye [18]. Carbon monoxide is an important toxic factor in non-flaming combustion as CO_2/CO is around 1, while this ratio becomes 10 in flaming combustion in some situations [18,19]. Maruf Hossain et al. [20] investigated biomass under non-flaming and flaming conditions and observed that CO emission ratio of non-flaming to flaming combustion is larger than 1.

Ventilation condition also show a significant effect on gas production. Experiments in cone calorimeter can be considered well-ventilated with an equivalence ratio between 0.7 and 1 [21]. Hietaniemi et al. [22] took experiments of several polymers in a controlled-atmosphere cone calorimeter. It was obtained that the amounts of CO_2 in the combustion fume decreased as the equivalence ratio increased, while the abundances of CO increased.

Non-charring polymers (HDPE, PP, PMMA) and charring polymers (ABS, PET, PC) were investigated in a cone calorimeter under autoignition conditions. The objectives of this study are:

- To investigate ignition time, heat release rate, mass loss rate and gas production of three thicknesses non-charring and charring polymers under autoignition condition;
- To compare heat of combustion and gas yields for polymers under autoignition and piloted ignition conditions;
- To compare gas yields for non-charring and charring polymers under non-flaming and flaming combustion; and
- To provide guidance for fire risk evaluation of non-charring and charring polymers under non-flaming and flaming combustion also modeling input or validation for numerical models under autoignition conditions.

2. Methodology

2.1. Materials

Six species of polymers including non-charring and charring polymers were chosen in experiments. Measured properties of polymer samples are listed in Table 1. All the tested polymers in the experiments were not flame-retarded. These tested polymers were originally in sheet form and were cut to desired size. Sample sizes are 100 × 100 mm with different thicknesses, namely 10, 20, and 30 mm. The data for thermal conductivity (λ) and specific heat capacity (C_P) come from Refs. [2,23].

2.2. Apparatus

Cone calorimeter (ISO 5660-1 [24]) as frequently used equipment for piloted ignition and autoignition was used in this study [25]. Polymer samples were put in horizontal orientation on specimen holder. External heat fluxes of 25, 50, and 75 kW/m^2 were chosen for this study, representing the low, middle and high external heat flux. Fig. 1 shows a view of sample in cone calorimeter.

2.3. Procedure

Before experiments, gas analyzers and external heat flux were first calibrated accordingly. Samples were then secured on a specimen holder and placed under the heater horizontally. The edges and rear surface of samples were covered with aluminum foil. Ceramic fibre blanket was used underneath sample for insulation. Protection screen was put down for protection. Change in weight was dynamically recorded using a build-in weighting device. A sample was considered ignited when visible flame was first observed. During experiments, the fan flow rate was kept at about 24 L/s. Spark plug was not used during whole experimental time. Each experiment was repeated at least two times. More runs were taken if the repeatability was not good.

3. Results and discussions

3.1. Analysis of raw data

It is a little difficult to define average mass loss rate ($\overline{MLR}$) during whole experimental time as they are sensitive to test end time. Lot of criteria were used to define test end time for cone calorimeter tests [26,27]. However, there are some limitations in specifying the test end time by these criteria, in particular for materials where it fails to ignite properly and then the *MLR* drops below 150 g/m^2 (average over a minute) [26].The *MLR* of non-charring polymers decrease dramatically at the end of test and

Table 1
Properties of tested polymers in this study.

Species	Material	ρ (kg/m^3)	λ (W/m K)	C_P (kJ/kg K)	Formula	[C] (%)
Non-charring	HDPE	971.3 ± 28.7	0.33	2.10	$-C_2H_4-$	85.7
	PP	938.6 ± 29.5	0.21	1.93	$-C_3H_6-$	85.7
	PMMA	1202.9 ± 38.5	0.21	1.46	$-C_5H_8O_2-$	60.0
Charring	ABS	1065.7 ± 40.2	0.26	1.50	$-C_8H_8 \cdot C_4H_6 \cdot C_3H_3N-$	85.3
	PET	1406.0 ± 27.3	0.20	1.15	$-C_{10}H_8O_2-$	62.5
	PC	1226.7 ± 20.0	0.20	1.22	$-C_{16}H_{14}O_3-$	75.6

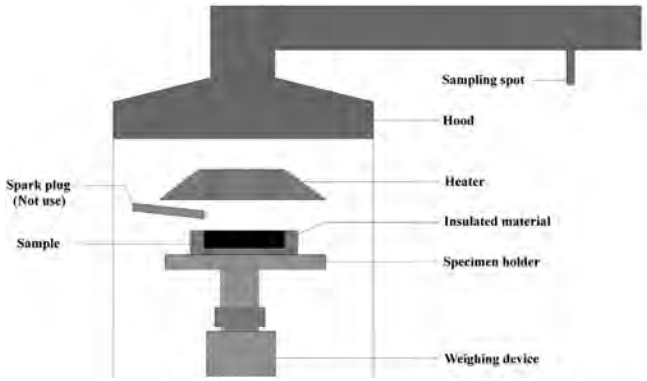

Fig. 1. A view of sample in cone calorimeter.

experiments may end in less than half an hour. But for some charring polymers, *MLR* decrease smoothly and time period may last more than an hour. Therefore, it seems difficult to set a unified criterion for both charring and non-charring polymers under non-flaming and flaming combustion. The $\overline{MLR}$ in this paper is then defined during a time period between experiment start and 50% mass loss. The $\overline{MLR}$ of wood samples has been well investigated in a cone calorimeter previously [14,15]. It can be obtained by

$$\overline{MLR} = 0.5\frac{m_0}{t_{50}} \tag{1}$$

where t_{50} is the time at 50% mass loss, s; and m_0 is the original mass of sample, s. The $\overline{MLR}$ in this study is different to normal $\overline{MLR}$, which may cover the main burning period of 10 to 90% mass loss.

Stoliarov et al. [28] defined average heat release rate ($\overline{HRR}$) of non-charring polymers by integrating an *HRR* curve from time to ignition to the time of final drop of *HRR* below 20 kW/m^2. This was to cut off part of the curve dominated by signal noise, which was notably higher in amplitude at the end of test than in the beginning. In this study, $\overline{HRR}$ of non-charring polymers were obtained following the same rule. Differently, charring polymers cannot burn out and non-flaming combustion still take place after flameout, resulting a higher *HRR*. So $\overline{HRR}$ of charring polymers was obtained between time to ignition and the time of final drop of *HRR* below 40 kW/m^2 or flameout, whichever was earlier.

3.2. Comparisons between charring and non-charring polymers

A summary of experimental results of polymers under auto-ignition conditions in a cone calorimeter is shown in Table 2. Key parameters, such as peak *HRR*, $\overline{HRR}$, time to peak *HRR*, $\overline{MLR}$, ignition time (t_{ig}), CO yield (y_{CO}) and CO_2 yield (y_{CO_2}) are provided for polymers under different external heat flux and thicknesses. The data at 25 kW/m^2 were not included in this table because of weak repeatability. According to ISO 17554 [29], experiment is need to be stopped manually if no ignition occurred after 30 or 32 min. Ignition of some polymers spread in a big time range even have not happened. This may be because the critical heat flux of these tested polymers are around 25 kW/m^2. The *HRR* history are not accurate as some polymers were not ignited during whole experimental time because they were so small to be measured. Except the *HRR* and ignition time, other experimental data can be seen in the following sections.

It is observed from Table 2 that differences exist between non-charring and charring polymers. This is partly because of their characteristics. Spearpoint and Quintiere [30] mentioned that non-charring materials burn away completely, but charring materials leave relatively significant amounts of residue.

The $\overline{HRR}$ for non-charring polymers are observed higher than those of charring polymers. In this aspect, it may be known that fire hazard of non-charring polymers are higher than those of charring polymers. Situations of CO yield (y_{CO}) are in an opposite way. The y_{CO} for charring polymers are observed higher than those for non-charring polymers. Differently, CO_2 yields (y_{CO_2}) performs under similar circumstance as $\overline{HRR}$. The y_{CO_2} for non-charring polymers are observed higher than those for charring polymers.

It is also observed that peak *HRR* and $\overline{HRR}$ of non-charring polymers increase with a higher heat flux or thickness. Luche et al. [4] obtained from experiments on black PMMA under piloted ignition condition that HRR depend strongly on irradiance level. This may because the burning of non-charring polymers can be considered as pool fire as all the solid polymer will melt at specific temperature. So reaction rate get higher as more heat are absorbed under high irradiance level, resulting in a higher HRR. Linteris et al. [31] also obtained a similar result of black PMMA that higher imposed heat fluxes lead to higher *HRR* and short ignition time. Spearpoint and Quintiere [10,30] mentioned that non-charring materials burn away completely leaving no residue and can be modeled using theory similar to flammable liquids.

For charring polymers, influences of sample thickness and external heat flux to peak and $\overline{HRR}$ seem to be much smaller than those of non-charring polymers. This may be because of the surface absorptivity, which decreases as temperature increasing [32]. Virginal polymer especially for char will block the penetration of heat under high temperature. The blocking effect becomes larger when the thickness of char layer increases. The increase of reaction rate under high irradiance for charring polymer would not be so obvious as non-charring polymer.

From Table 2, it is known that time to peak *HRR* increases with a higher thickness or a lower external heat flux for both of non-charring and charring polymers. This phenomenon happens because *HRR* is highly related to pyrolysis reaction which is largely dependent on temperature. For high thickness sample, temperature inside solid phase rises much slowly when polymers are put under the same heat flux. It costs more time for the whole slab to reach the same temperature level. The reason why time to peak *HRR* increases with a lower heat flux can be explained in the same way.

3.3. Autoignition time and thermal thickness

Ignition time of combustible materials are affected by their thermal thickness. A material is classified as 'thermal thin' when the heat from the fire (otherwise known as the thermal wave) is

Table 2
A summary of experimental results under autoignition conditions in cone calorimeter.

Material	Thickness (mm)	Heat flux (kW/m^2)	Peak *HRR* (kW/m^2)	$\overline{HRR}$ (kW/m^2)	Time to peak *HRR* (s)	$\overline{MLR}$ (g/m^2 s)	t_{ig}(s)	y_{CO}(g/g)	y_{CO2}(g/g)
HDPE	10	50	550	240	350	12	78	0.027	2.11
	20	50	480	280	890	14	68	0.023	1.74
	30	50	920	410	1430	14	66	0.027	2.59
	10	75	870	340	300	16	33	0.047	3.19
	20	75	1130	460	580	18	30	0.035	2.61
	30	75	1100	480	890	24	28	0.037	2.18
PP	10	50	510	270	300	11	43	0.035	2.47
	20	50	590	330	230	15	39	0.028	2.02
	30	50	1080	420	1030	15	35	0.056	3.49
	10	75	890	450	290	18	22	0.048	2.97
	20	75	930	530	560	18	18	0.058	3.37
	30	75	1550	730	850	22	17	0.075	4.50
PMMA	10	50	980	440	420	18	52	0.018	2.97
	20	50	950	520	890	20	37	0.019	3.46
	30	50	880	570	1370	21	32	0.020	3.47
	10	75	1110	580	310	26	24	0.022	3.40
	20	75	1150	690	610	27	19	0.019	2.91
	30	75	1470	710	870	31	17	0.026	3.10
ABS	10	50	970	450	430	17	49	0.11	3.21
	20	50	810	530	830	19	41	0.10	2.89
	30	50	690	430	240	21	23	0.11	3.55
	10	75	1030	560	320	26	21	0.14	3.13
	20	75	970	560	600	30	19	0.11	2.41
	30	75	800	410	110	31	13	0.11	2.83
PET	10	50	370	120	350	12	88	0.071	2.18
	20	50	390	150	180	10	107	0.049	1.62
	30	50	410	130	160	10	89	0.035	1.74
	10	75	410	160	110	19	34	0.022	0.81
	20	75	540	200	90	15	32	0.035	1.89
	30	75	450	130	60	14	30	0.022	1.30
PC	10	50	410	180	170	9.4	101	0.091	2.04
	20	50	430	180	160	6.8	127	0.096	2.37
	30	50	460	160	260	5.7	146	0.099	2.32
	10	75	400	180	140	13	38	0.074	2.23
	20	75	450	160	70	9.9	30	0.051	2.34
	30	75	430	140	90	7.4	29	0.045	1.87

absorbed so rapidly that there is no significant temperature gradient through it. In a 'thermal thick' material, by contrast, a significant temperature gradient exists through the materials [33].

Thermal penetration depth at ignition (δ_P) can be considered as thermal thickness for a material. For a one-dimensional slab, thermal penetration depth can be defined as the thickness of the sample which has been heated to a certain temperature [2]. If the thickness of a sample is larger than δ_P, temperature gradient exits as thermal wave has not reached the bottom at ignition. Bottom part of the slab are still at ambient temperature as they have not been heated yet. When sample thickness is less than δ_P, thermal wave reaches the bottom and reflects back before ignition, and temperature gradient inside the whole slab is small. Samples can be then considered thermal thin. And δ_P is usually defined as [2]

$$\delta_P = A\sqrt{\frac{\lambda t_{ig}}{\rho C_p}} \tag{2}$$

where A is a coefficient which changes from one author to another. Mikkola and Wichman [33,34] used a constant of 1. And a value of 1.2 was offered by Dusinberre [35]. Babrauskas [2] suggested that a value of 1.13 is more appropriate, which will be used in this study.

Babrauskas [2] made calculations for various densities and heat fluxes and suggested that for particle board a minimum thickness required to insure that that the specimen is thermal thick can be represented by

$$\delta_P = 0.6\frac{\rho}{\dot{q}''} \quad \text{(wood)} \tag{3}$$

Eq. (3) is used to estimate thermal thickness of particle board under heat flux. Parameters such as density and heat flux, which are easy to be obtained, are used in this model. Thermal thickness of polymers may follow a similar trend that they are proportional to $\rho/\dot{q}''$.

Fig. 2 shows comparisons of autoignition time among three sample thicknesses. Although big difference exists for ABS between 10 and 20 mm thickness, it may still be obtained that autoignition time decrease with a higher sample thickness from statistics analysis of all tested polymers. But the influences to autoignition time are not obvious. This may indicate that all tested samples in this study can be considered thermal thick. However, according to data in this study, Eq. (3) seems to be inappropriate as this empirical model was originally developed based on experimental data of wood products. Predictions by this model are higher than practice when it is applied to polymers.

Polymers' thermal thicknesses can be calculated by Eq. (2) using ignition time and other thermal properties shown in Table 1. The δ_P for polymers may follow a similar trend with Eq. (3) that they are proportional to $\rho/\dot{q}''$. Fig. 3 shows a correlation between δ_P and $\rho/\dot{q}''$. It is observed that these two fits well. The δ_P of polymers under autoignition conditions can be estimated by

$$\delta_P = 0.14\frac{\rho}{\dot{q}''} \quad \text{(polymer)} \tag{4}$$

In Eq. (3), a model with a coefficient of 0.6 is used to predict thermal thickness of wood products under piloted ignition condition. This model is useful as it uses easy-to-get parameters namely

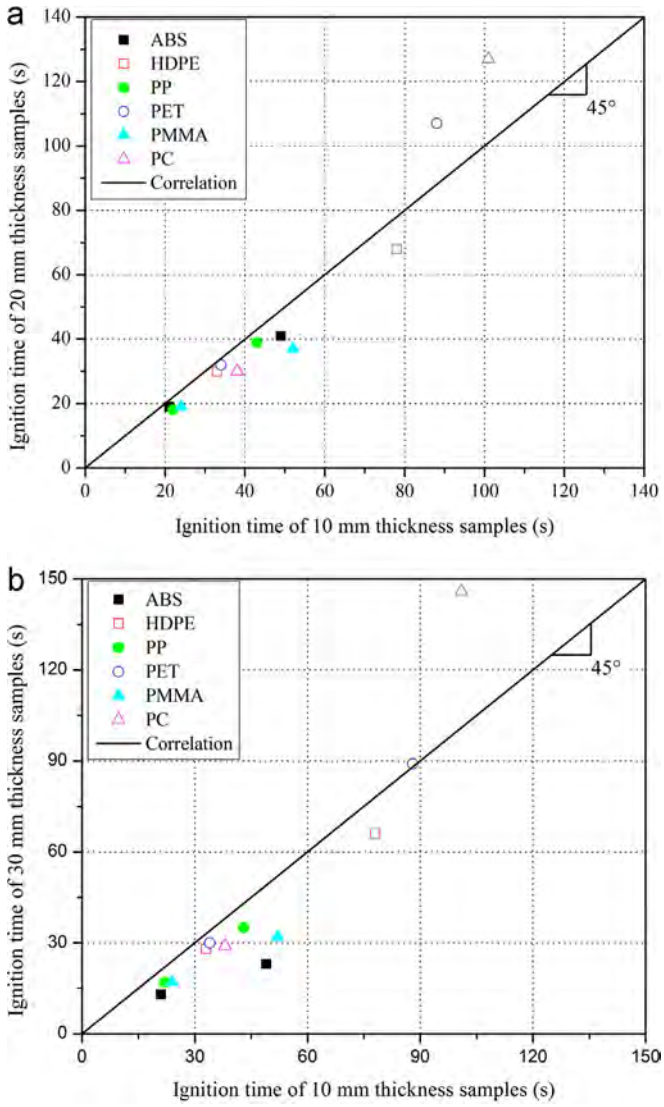

Fig. 2. Comparisons of autoignition time among difference sample thicknesses.

density and heat flux for input. However, predictions by this model are higher than practice when it is applied to polymers. So a model with coefficient of 0.14 is suggested for the prediction of polymers' thermal thickness under autoignition conditions.

It is observed from Fig. 4 that heat flux has significant influences to autoignition time. Ignition time decrease dramatically with a higher external heat flux. Autoignition time of charring polymers seem to be more sensitive to external heat flux comparing to non-charring polymers. Correlations can be obtained for charring and non-charring polymers, respectively

$$\begin{cases} t_{ig,75} = 0.45 t_{ig,50} & \text{non-charring polymer} \\ t_{ig,75} = 0.29 t_{ig,50} & \text{charring polymer} \end{cases} \quad (5)$$

3.4. Heat release characteristics

3.4.1. Heat release rate

Non-charring and charring polymers show different characteristics of *HRR*, seen in Fig. 5. For non-charring polymer, peak *HRR* happen near test end. Tewarson [36] obtained a similar result. He divided the *HRR* history of PP into three stages: solid stage, molten stage, and boiling liquid stage. And peak *HRR* shows at the last stage, namely boiling liquid stage. Schartel et al. [37] interpreted

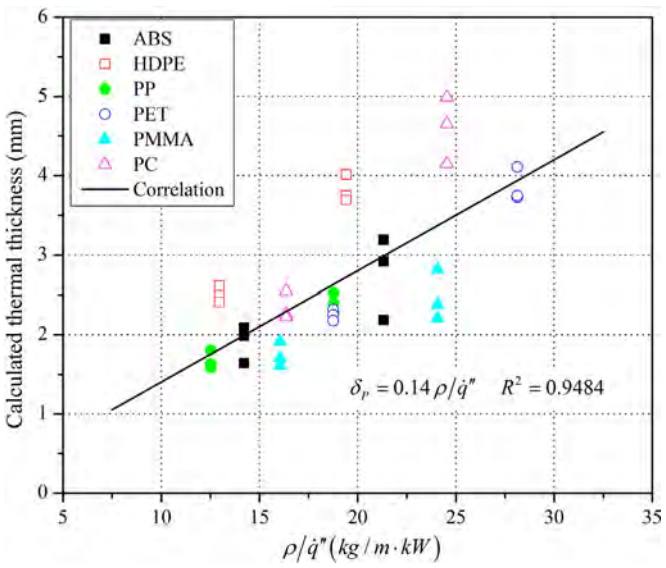

Fig. 3. A correlation between thermal thickness and other properties.

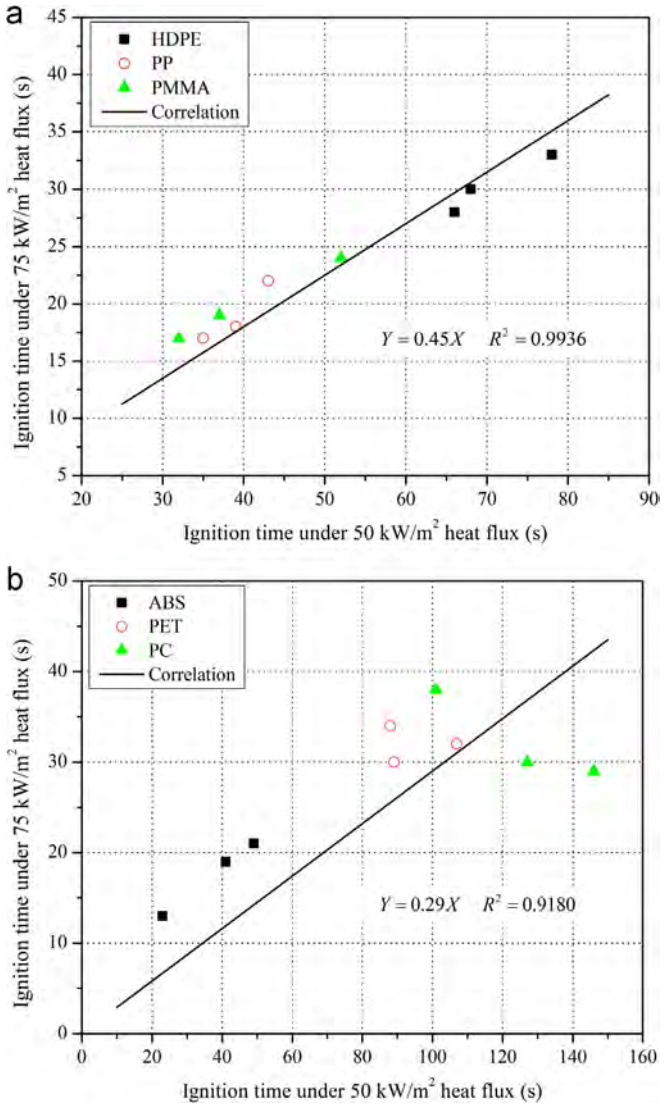

Fig. 4. Influences of external heat flux to autoignition time for: (a) non-charring polymers and (b) charring polymers.

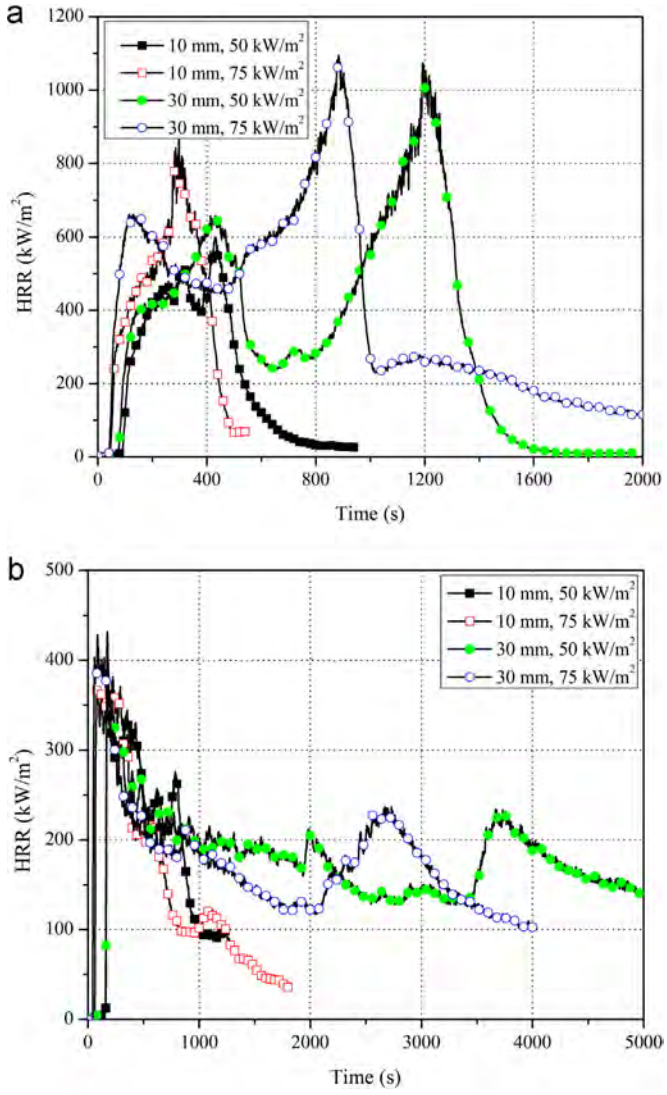

Fig. 5. *HRR* history under external heat flux for: (a) HDPE and (b) PC.

that a peak of *HRR* at the end of burning phase is caused by thermal feedback that occurs when the pyrolysis zone reaches the back of the sample. Schartel and Hull [21] also mentioned that this peak is caused by diminution of conductive heat as insulated material supporting sample prevents heat transfer to specimen holder as pyrolysis zone approaches it.

As mentioned in Section 3.2, $\overline{HRR}$ for non-charring polymers are sensitive to heat flux and sample thickness. This phenomenon for *HRR* history also can be seen in Fig. 5. Luche et al. [4] obtained that the *HRR* of black PMMA under piloted ignition condition depend strongly on irradiance level. Linteris et al. [31] also obtained a similar result for black PMMA that higher imposed heat fluxes lead to higher *HRR* and short ignition times. This may be because the burning of non-charring polymers can be considered as pool fire as all the solid polymer will melt at specific temperature. So reaction rate get higher as more heat are absorbed under high irradiance level, resulting in a higher *HRR*. Spearpoint and Quintiere [10,30] mentioned that non-charring materials burn away completely leaving no residue and can be modeled using theory similar to flammable liquids.

For charring polymers, it is observed from Fig. 5 that peak *HRR* happens shortly after ignition. From Table 2, it is also noticed that the influence of heat flux to peak *HRR* is not obvious as non-charring polymers. This may be because of the surface absorptivity, which decreases as temperature increasing [32]. Virginal polymer especially for char will block the penetration of heat under high temperature. The blocking effect becomes larger when the thickness of char layer increases. Schartel et al. [37] also mentioned that char and residue-forming materials immediately show a peak of *HRR* after the initial strong increase in the *HRR* due to the formation of a protective surface layer.

The *HRR* curves of charring polymers are not repeatable as non-charring polymers. Stoliarov et al. [38] observed the same phenomena when they took experiments on PC and PVC in cone calorimeter. Volume of PC increases dramatically after ignition, and increasing rate goes down until test end. Expanded char has influences to the *HRR* because of its influence to pyrolysis reaction. As the char expanding, distance between surface and bottom increases, then temperature at the bottom side increases slowly as more time is needed for heat transportation from surface. Another reason may be because of influence from other fire damages, such as pore formation, delamination cracking, and matrix cracking [39].

Table 3
Comparisons of average *EHC* between autoignition and piloted ignition.

Materials	*Average EHC* (kJ/g)		Reference data by piloted ignition[a]
	$\dot{q}''=50$ kW/m^2	$\dot{q}''=75$ kW/m^2	
HDPE	28.4	25.5	30.0(35) [42]; 40.3 [23];
PP	27.1	26.6	34.0(35) [42]; 41.9 [23];
PMMA	25.5	21.3	22.4(50) [27]; 23.3(20–60) [43]; 24.6(50) [4]; 24.8[23]
ABS	29.0	24.6	28.2(20–60) [43]; 29.0 [23]; 30.0(50) [44];
PET	18.3	18.0	18.0 [23];
PC	25.5	23.0	21.2 [23]; 23.0(35) [42];

[a] The data in bracket present heat flux, kW/m^2. No mention means no information was provided in references.

3.4.2. Heat of combustion

Average chemical heat of combustion determined in cone calorimeter is defined as effective heat of combustion (*EHC*) [36]. *EHC* is the heat of combustion which would be expected in a fire where incomplete combustion takes place. This amount is less than theoretical heat of combustion as measured in the oxygen bomb calorimeter [40].

EHC is a time- and irradiance-level-dependent parameter that corresponds to the heat released from the volatile portion during solid material combustion, which can be computed using the following equation [4]

$$EHC = \frac{HRR}{MLR} \tag{6}$$

Table 3 compared average *EHC* in this study and the data from references under piloted ignition conditions. It is noticed for non-charring polymers that differences exist between these two. Average *EHC* under autoignition conditions are observed lower than those reference data under piloted ignition conditions. There is an exception of PMMA, difference of average *EHC* under piloted ignition and autoignition conditions is not obvious. It may be indicated that ignition method has influence to the *EHC* for non-charring polymers. Lyon and Janssens [23] mentioned the *EHC* is determined primarily by the fuel chemistry, ventilation rate, and combustion efficiency in the flame. Hull et al. [41] also mentioned that *EHC* is a function of the dynamics of the fire and combustion efficiency. The difference for HDPE and PP may be because ignition method has influence to the combustion efficiency.

For charring polymers in this study, little difference can be observed with those under piloted conditions. According to this

point, it may indicate that the influence of ignition method to the combustion efficiency can be ignored for charring polymers.

3.5. Mass loss rate

Fig. 6 shows *MLR* history of polymers. For non-charring polymer such as PP, peak *MLR* increases under a higher radiance. This phenomenon is similar to those of *HRR*. Luche et al. [4] obtained that the *HRR* of black PMMA under piloted ignition condition depend strongly on irradiance level. Linteris et al. [31] also obtained a similar result for black PMMA that higher imposed heat fluxes lead to higher *HRR* and short ignition times. This may be because the burning of non-charring polymers can be considered as pool fire as all the solid polymer will melt at specific temperature. So reaction rate get higher as more heat are absorbed under high irradiance level, resulting in a higher *HRR*.

Peak *MLR* of non-charring polymers also rises with a bigger sample thickness. Tewarson [36] observed that *HRR* history can be divided into three stages and peak *HRR* happens at the last stage namely liquid boiling stage. This phenomenon was interpreted by Schartel et al. [37] that it is caused by thermal feedback that occurs when the pyrolysis zone reaches the back of the sample. During the boiling stage, burning rate keeps increasing before burning out because of thermal feedback from the bottom. This is the reason why a higher thickness sample shows a higher peak *MLR*. This is also can be used to explain why time to peak *MLR* decreases with a higher heat flux or a lower thickness.

For charring polymers, influence of heat flux to peak *MLR* is similar to that of non-charring polymers. For charring polymers, peak *MLR* also increases dramatically when heat flux increase from 25 to 50 kW/m^2. But the increase is not so obvious when heat flux increases from 50 to 75 kW/m^2. This is because the formation of char layer which block the penetration of heat from outside.

Comparisons of $\overline{MLR}$ under different irradiances are shown in Fig. 7. It is observed that $\overline{MLR}$ increases with a higher external heat flux. $\overline{MLR}$ increase linearly when heat flux rise from 50 to 75 kW/m^2. $\overline{MLR}$ increases about 50% when irradiance rises from 50 to 75 kW/m^2. Luche et al. [4] obtained a similar result that average specific *MLR* of black PMMA increase linearly with heat flux by piloted ignition in a cone calorimeter. In their study, specific *MLR* were determined as the ratio between the *MLR* and exposed surface area. Average specific *MLR* were calculated between experiment start and burning out of PMMA. It is worth notice that increasing rate of average specific *MLR* under different heat flux was different from this study because data were obtained under different situations.

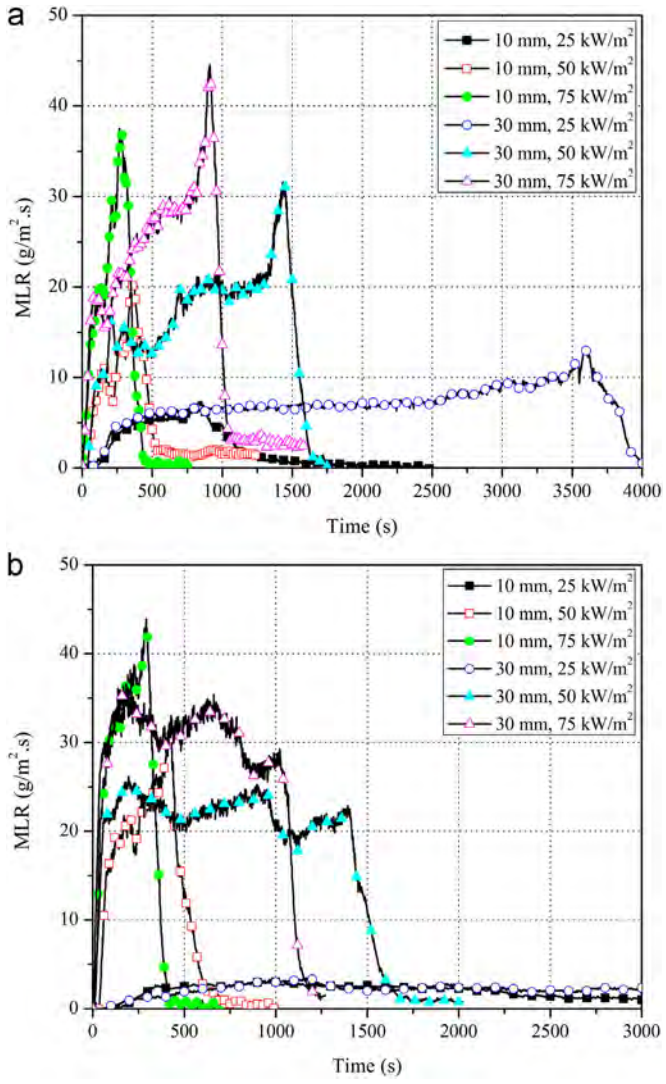

Fig. 6. *MLR* history under external heat flux for (a) PP and (b) ABS.

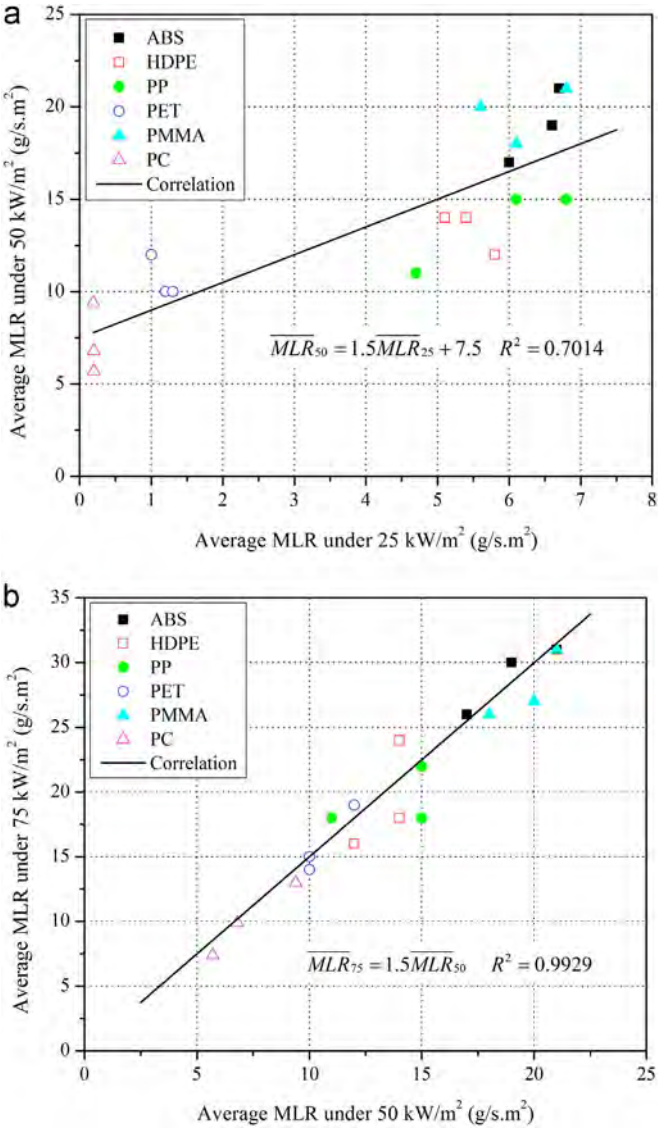

Fig. 7. Comparisons of average *MLR* under different heat flux.

From Fig. 7, it is observed that correlation for $\overline{MLR}$ between 25 and 50 kW/m^2 does not sound well. This is because polymers such as PET and PC go through non-flaming combustion as they were not ignited under low irradiance level. For ABS, HDPE, PP and PMMA, it takes a long time to be ignited and some of them are even longer than half an hour. These polymers mainly go through non-flaming combustion. Flaming combustion is the main process for polymers under 50 kW/m^2 heat flux. This may be also the reason that a correlation with intercept was obtained.

Relationship of $\overline{MLR}$ under different heat flux can be estimated

$$\overline{MLR}_{50} = 1.5\overline{MLR}_{25} + 7.5 \tag{7}$$

$$\overline{MLR}_{75} = 1.5\overline{MLR}_{50} \tag{8}$$

3.6. Gas release rate and gas yield

3.6.1. Gas yields under non-flaming and flaming conditions

Production process of CO and CO_2 for polymers can be simply considered as a two-steps reaction [32]. Carbon monoxide including other gas volatiles are produced during first step pyrolysis reaction, which can be expressed by Arrhenius Law. The second step is oxidation reaction of CO if enough oxygen is avaible. The whole process is expressed by

$$\begin{cases} \text{Step 1}: \ \text{Polymer} + O_2 \rightarrow H_2O + CO + \text{others products} \\ \text{Step 2}: \ CO + 0.5O_2 \rightarrow CO_2 \end{cases} \tag{9}$$

Although many previous studies [4,45–47] have focused on CO yield (y_{CO}) and CO_2 yield (y_{CO_2}) under different ventilation, few studies have been taken about the comparisons of yields under non-flaming and flaming conditions. The comparisons are possible in this study is because the autoignition under 25 kW/m^2 heat flux takes a long time, and some of them even longer than half an hour. This is because no acceleration for ignition exist as spark plug was not used during the whole experimental time.

Table 4 shows y_{CO} and y_{CO_2} of polymers under non-flaming and flaming combustion combustions. A point is needed to be mentioned that these data were obtained under 25 kW/m^2. Yields were obtained by mass loss and gas production during non-flaming and flaming conditions in which ignition was considered as demarcation point. Data from high irradiances of 50 and 75 kW/m^2 were excluded because mass loss during non-flaming combustion were not obvious as ignition happened shortly after test start.

Yield of CO_2 increase dramatically when non-flaming transitions to flaming combustion. It is noticed that y_{CO_2} increases at least 40 times. For charring polymer such as ABS, y_{CO_2} are significantly affected, which increases about 170 times. Reason of this phenomenon may be similar to that of woods [17]. Oxidation reaction of CO, namely step 2 in Eq. (9), was accelerated when visible flame is presented. Under flaming combustion, temperature inside solid phase will increase more rapidly because of flame heat flux. Oxidation reaction rate are higher under high temperatures. A large amount of CO_2 are then produced under this situation.

It is noticed from Table 4 that y_{CO} also increases when non-flaming transitions to flaming combustion. The y_{CO} of ABS, PP and PMMA increase about 30, 1.5 and 2.9 times, respectively. This may be because of the high reaction rate of step 1 in Eq. (9). Although some part of CO change into CO_2 under step 2, oxidation reaction still is limited by the oxygen level. For these polymers, more CO are produced because pyrolysis reaction of original polymer is much significant than oxidation reaction. There is an exception of HDPE. The y_{CO} of HDPE decreases as non-flaming transitions to flaming combustion, which is similar to that of woods [17,48].

Table 4
Yields of CO and CO_2 under non-flaming and flaming combustion.

Material	Non-flaming combustion		Flaming combustion		Ratio (y'/y'')	
	y'_{CO}	y'_{CO_2}	y''_{CO}	y''_{CO_2}	CO	CO_2
HDPE	0.12	0.052	0.021	1.99	1:0.18	1:40
PP	0.02	0.037	0.03	2.16	1:1.5	1:60
PMMA	0.007	0.04	0.02	2.00	1:2.9	1:50
ABS	0.0028	0.016	0.086	2.71	1:30	1:170
PET[a]	0.09	0.09	–	–	–	–
PC[a]	0.19	0.74	–	–	–	–

[a] Visible flame were not observed during whole experimental time when they were put under 25 kW/m^2 heat flux. So it is considered that these samples only go through non-flaming combustion.

3.6.2. Gas yields under autoignition and piloted ignition conditions

The y_{CO} under autoignition condition were observed different from reference data under piloted ignition condition. Comparisons of y_{CO} under two conditions are shown in Table 5. It is worth mentioned that y_{CO} in this study were calculated during whole experimental time. It is observed that y_{CO} are higher than reference data. The y_{CO} of polymers such as ABS, PP and PMMA are higher than reference data. For HDPE and PC, y_{CO} seem to be higher than reference data even one date is close to reference data. No comparison was taken for PET as no reference data has been found. It is known from Eq. (9) that y_{CO} is largely depended on both pyrolysis reaction of original material and oxidation of CO. The reason why y_{CO} are higher than reference data is not clear so far.

The y_{CO_2} are compared with reference data under piloted ignition condition, shown in Table 6. No rule has been found between these two. The y_{CO_2} of ABS and PC, y_{CO_2} are higher than reference data. For other polymers, the y_{CO_2} seem to be lower than reference data. No comparison was taken for PET as no reference data has been found. For PMMA, the data is much higher than theoretical maximum data may be because of measurement error.

3.6.3. Influences of heat flux to gas yields

Experimental results showed that y_{CO} and y_{CO_2} are dependent on heat flux. Fig. 8 shows comparisons of y_{CO} and y_{CO_2} under 50 and 75 kW/m^2. For tested non-charring polymers, it is observed that y_{CO} increase under higher irradiance. This may be because of the ventilation in experiments. Pyrolysis reaction of polymers, namely step 1 in Eq. (9), will increase as temperature rises under high heat flux. Oxidation reaction of CO is limited as the limitation of ventilation condition. This may be the reason why y_{CO} increase under higher irradiance. The trend for charring polymers is not clear. The trends of y_{CO} for charring polymers may be dependent on the needs of oxygen under limited ventilation condition.

Table 5
Comparisons of CO yield between autoignition and piloted ignition.

Materials	y_{CO} (g/g)		Reference data by piloted ignition[a]
	$\dot{q}''=50$ kW/m^2	$\dot{q}''=75$ kW/m^2	
HDPE	0.025	0.040	0.017(25) [45]; 0.018(40) [45]; 0.024 [36]
PP	0.040	0.060	0.024 [36];
PMMA	0.019	0.022	0.005(30) [45]; 0.0058(50) [27]; 0.006(50) [4]
ABS	0.11	0.12	0.056(20) [45]; 0.057(30) [45]
PET	0.052	0.026	–
PC	0.095	0.057	0.054 [36]

[a] The data in bracket present heat flux, kW/m^2. No mention means no information was provided in references.

Table 6
Comparisons of CO_2 yield between autoignition and piloted ignition.

Materials	y_{CO_2} (g/g)		Reference data[a]	Theoretical maximum CO_2 yield
	$\dot{q}''=50$ kW/m^2	$\dot{q}''=75$ kW/m^2		
HDPE	2.15	2.66	2.90(25,40) [45]; 2.76 [36];	3.14
PP	2.66	3.61	2.79 [36]	3.14
PMMA	3.30	3.14	2.2(15) [45]; 2.30(30) [45]; 1.98(50) [27]; 2.22(50) [4]	2.20
ABS	3.22	2.79	2.40(20,30) [45];	3.13
PET	1.84	1.34	–	2.29
PC	2.25	2.15	1.5 [36]	2.77

[a] The data in bracket present heat flux, kW/m^2. No mention means no information was provided in references.

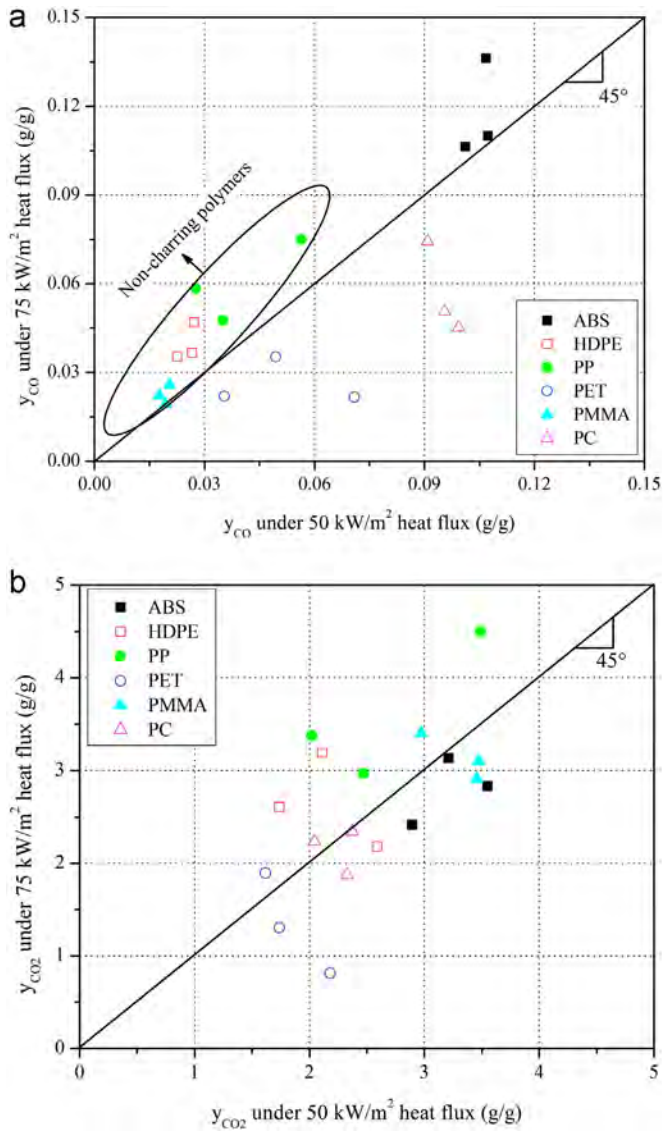

Fig. 8. Comparisons of gas yields under 50 and 75 kW/m^2 for (a) CO and (b) CO_2.

Shown in Fig. 8, no big difference of y_{CO_2} is observed under two heat flux increases. The irradiance seems to have limited influence to y_{CO_2}. Under flaming combustion, y_{CO_2} increases dramatically because of the acceleration of CO oxidation reaction at the presence of visible flame. It is obtained that visible flame may have the similar effect to CO_2 production.

Fig. 9 shows y_{CO}/y_{CO_2} of polymers under two irradiances. For non-charring polymers, y_{CO}/y_{CO_2} was observed to increase with a higher irradiances. This is because y_{CO} increase with a higher

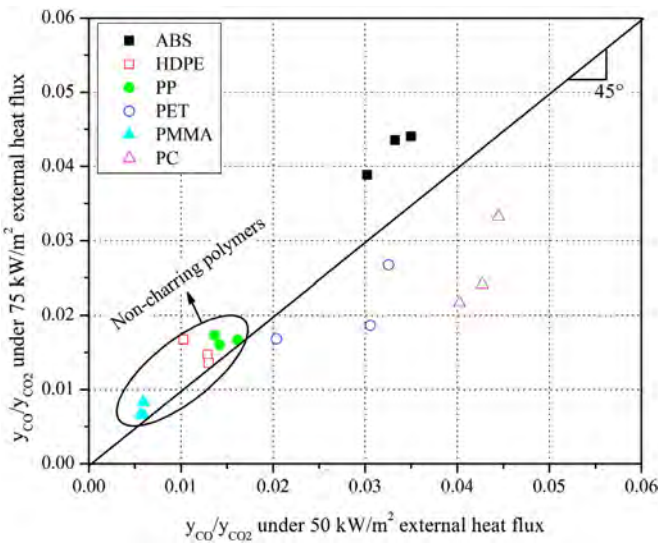

Fig. 9. Comparison of y_{CO}/y_{CO_2} under heat flux.

irradiance, and irradiance has limited influence to CO_2 production. Similarly, no trend is found for charring polymers.

3.6.4. *Influences of mass percent of carbon to gas yields*

Fig. 10 shows comparisons of y_{CO} and y_{CO_2} under six situations, namely three sample thicknesses (10, 20 and 30 mm) and two heat flux (50 and 75 kW/m^2). In this study, gas yield of one polymer was considered higher than the other if it have higher gas yields under most of the situations. Sequences of y_{CO} and y_{CO_2} from highest to lowest are

$$\begin{cases} y_{CO}: & \text{ABS} > \text{PC} > \text{PP} > \text{PET} > \text{HDPE} > \text{PMMA} \\ y_{CO_2}: & \text{PMMA} > \text{ABS} > \text{PP} > \text{HDPE} > \text{PC} > \text{PET} \end{cases} \quad (10)$$

From formula (10), it is noticed that charring polymers seem to have higher y_{CO} than those of non-charring polymers. Charring polymers such as ABS, PC and PET have the highest, second highest and fourth highest y_{CO}, respectively. The y_{CO_2} of non-charring polymers were observed higher than those of charring polymers.

From Table 1, sequence of mass percent of carbon is

$$[C]: \quad \text{HDPE} = \text{PP} > \text{ABS} > \text{PC} > \text{PET} > \text{PMMA} \quad (11)$$

Comparing formula (10) with (11), it is noticed that mass percent of carbon has little influence to y_{CO} and y_{CO_2}. For example, HDPE have the highest mass percent of carbon, but its y_{CO} and y_{CO_2} are lower than ABS. Schartel and Hull [21] have a similar statement that both CO production and smoke production result from incomplete combustion, which are strongly dependent on the material. In this study, it is observed from experiments that the

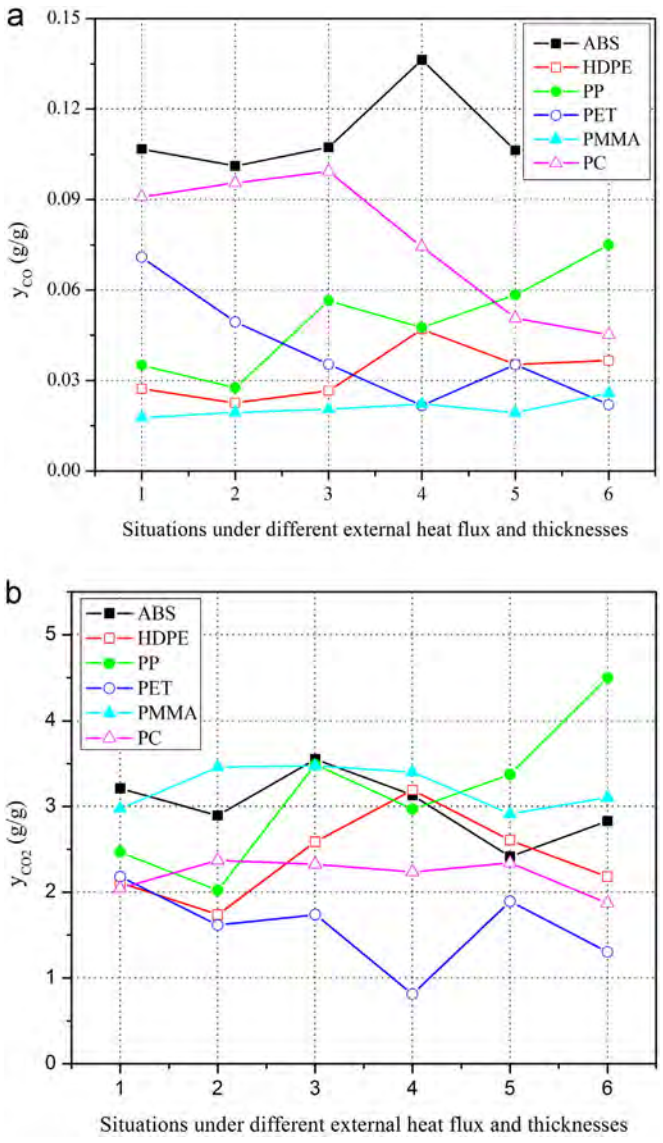

Fig. 10. Comparisons of gas yields under different situations for: (a) CO and (b) CO_2.

productions of CO and CO_2 are strongly dependent on materials, not the mass percent of carbon.

4. Conclusions

This paper investigated fire behaviors of non-charring and charring polymers under autoignition conditions in a cone calorimeter. Ignition time, mass loss rate, heat release rate, gas yields, thermal thickness, and effective heat of combustion were included. The following conclusions can be addressed:

(1) Autoignition time decrease dramatically with a higher heat flux. Charring polymers seem to be more sensitive to heat flux comparing to non-charring polymers. An empirical model was obtained to predict thermal thickness of polymers by using density and heat flux.
(2) Fire risk of non-charring polymers are higher than those of charring polymers because of high heat release, and the increase of heat release rate is much obvious with a higher heat flux or thickness. The burning of non-charring polymers performs like pool fire as melting happens at specific temperature. For charring polymer, char layer will block the penetration of heat, resulting in small change under high irradiance.
(3) Ignition methods have influences to combustion efficiency of non-charring polymers as effective heat of combustion under autoignition are observed lower than those reference data under piloted ignition conditions. But the influence to charring polymers can be ignored. Carbon monoxide yields under autoignition were observed higher than those under piloted ignition condition.
(4) Production process of CO and CO_2 can be considered as a two-step reaction: pyrolysis reaction of polymer and oxidation reaction of CO. Both CO and CO_2 yields under flaming combustion are higher than those under non-flaming combustion. Charring polymers seem to have a higher CO yield, while non-charring polymers have a higher CO_2 yield. The CO yield of tested non-charring polymers increase under higher irradiance, and trend for charring polymers is not clear. Mass percent of carbon has limited effect to CO and CO_2 yield, which are strongly dependent on materials.

Fire behaviors of polymers are sensitive to environmental conditions. Experimental data in this study can provide a guidance to fire risk evaluation of non-charring and charring polymers. Also it can be used for modeling input or validation of numerical models under autoignition conditions.

References

[1] D. Drysdale, Ignition: the initiation of flaming combustion, An Introduction to Fire Dynamics, third ed., Wiley (2011) 225–275. (Chapter 6).
[2] V. Babrauskas, Ignition Handbook: Principles and Applications to Fire Safety Engineering, Fire Investigation, Risk Management and Forensic Science, Fire Science Publishers, 2003.
[3] P. Mindykowski, A. Fuentes, J.L. Consalvi, B. Porterie, Piloted ignition of wildland fuels, Fire Safety Journal 46 (2011) 34–40.
[4] J. Luche, T. Rogaume, F. Richard, E. Guillaume, Characterization of thermal properties and analysis of combustion behavior of PMMA in a cone calorimeter, Fire Safety Journal 46 (2011) 451–461.
[5] S. McAllister, C. Fernandez-Pello, D. Urban, G. Ruff, Piloted ignition delay of PMMA in space exploration atmospheres, Proceedings of the Combustion Institute 32 (2009) 2453–2459.
[6] D. Rich, C. Lautenberger, J.L. Torero, J.G. Quintiere, C. Fernandez-Pello, Mass flux of combustible solids at piloted ignition, Proceedings of the Combustion Institute 31 (2007) 2653–2660.
[7] R.E. Lyon, J.G. Quintiere, Criteria for piloted ignition of combustible solids, Combustion and Flame 151 (2007) 551–559.
[8] M.A. Delichatsios, Piloted ignition times, critical heat fluxes and mass loss rates at reduced oxygen atmospheres, Fire Safety Journal 40 (2005) 197–212.
[9] Y.Y. Zhou, D.C. Walther, A.C. Fernandez-Pello, Numerical analysis of piloted ignition of polymeric materials, Combustion and Flame 131 (2002) 147–158.
[10] M.J. Spearpoint, J.G. Quintiere, Predicting the piloted ignition of wood in the cone calorimeter using an integral model-effect of species, grain orientation and heat flux, Fire Safety Journal 36 (2001) 391–415.
[11] B. Moghtaderi, V. Novozhilov, D.F. Fletcher, A new correlation for bench-scale piloted ignition data for wood, Fire Safety Journal 29 (1997) 41–59.
[12] Melinek S.J., Fire Research Note 755 Ignition Behaviour of Heated Wood Surfaces, Fire Research Station, 1969.
[13] V. Babrauskas, Ignition of wood: a review of the state of the art, Journal of Fire Protection Engineering 12 (2002) 163–189.
[14] L. Shi, M.Y.L. Chew, Influence of moisture on autoignition of woods in cone calorimeter, Journal of Fire Sciences 30 (2012) 158–169.
[15] L. Shi, M.Y.L. Chew, Experimental study of woods under external heat flux by autoignition: ignition time and mass loss rate, Journal of Thermal Analysis and Calorimetry 111 (2013) 1399–1407.
[16] M.W. Cain, IR/L/FR/85/10 an investigation into the ignitability characteristics of several common materials, Health and Safety Executive, UK (1985).
[17] L. Shi, M.Y.L. Chew, Experimental study of carbon monoxide for woods under spontaneous ignition condition, Fuel 102 (2012) 709–715.
[18] G. Rein, Smoldering combustion phenomena and coal fires, Coal and Peat Fires: A Global Perspective, Elsevier (2011) 307–315. (Chapter 17).
[19] D.A. Purser, Toxicity assessment of combustion products, SFPE Handbook of Fire Protection Engineering, National Fire Protection Association, Quincy (2002) 2.83–2.171. (Chapter 2–6).
[20] A.M.M. Maruf Hossain, S. Park, J.S. Kim, K. Park, Volatility and mixing states of ultrafine particles from biomass burning, Journal of Hazardous Materials 205–206 (2012) 189–197.

[21] B. Schartel, T.R. Hull, Development of fire-retarded materials—interpretation of cone calorimeter data, Fire and Materials 31 (2007) 327–354.
[22] J. Hietaniemi, R. Kallonen, E. Mikkola, Burning characteristics of selected substances: production of heat, smoke and chemical species, Fire and Materials 23 (1999) 171–185.
[23] R.E. Lyon, M.L. Janssens, Flammability, Encyclopedia of Polymer Science and Technology, John Wiley & Sons, Inc. (2005) 1–73.
[24] ISO 5660-1, Reaction to Fire Tests – Heat Release, Smoke Production and Mass Loss Rate – Part 1 Heat Release Rate (Cone Calorimeter Method), 2002.
[25] Fire Testing Technology Limited, West Sussex, UK, 2001.
[26] P.C.R. Collier, P.N. Whiting, C.A. Wade, BRANZ Study Report SR 160 Fire Properties of Wall and Ceiling Linings: Investigation of Fire Test Methods for Use in NZBC Compliance Documents, Branz Ltd, New Zealand, 2006.
[27] K.T. Paul, Cone calorimeter: initial experiences of calibration and use, Fire Safety Journal 22 (1994) 67–87.
[28] S.I. Stoliarov, S. Crowley, R.E. Lyon, G.T. Linteris, Prediction of the burning rates of non-charring polymers, Combustion and Flame 156 (2009) 1068–1083.
[29] ISO 17554, International Standard—Fire Tests—Reaction to Fire—Mass Loss Measurement, 1998.
[30] M.J. Spearpoint, J.G. Quintiere, Predicting the burning of wood using an integral model, Combustion and Flame 123 (2000) 308–324.
[31] Linteris G., Gewuerz L., McGrattan K., Forney G., Modeling solid sample burning, in: The Eighth International Symposium on Fire Safety Science, 2005, pp. 625–636.
[32] L. Shi, M.Y.L. Chew, A review of fire processes modeling of combustible materials under external heat flux, Fuel 106 (2013) 30–50.
[33] A.P. Mouritz, A.G. Gibson, Fire reaction properties of composites, Fire Properties of Polymer Composite Materials, Springer (2006) 59–101. (Chapter 3).
[34] E. Mikkola, I.S. Wichman, On the thermal ignition of combustible materials, Fire and Materials 14 (1989) 87–96.
[35] G.M. Dusinberre, Heat Transfer by Finite Difference Methods, Wiley, 1961.
[36] A. Tewarson, Generation of heat and chemical compounds in fires, SFPE Handbook of Fire Protection Engineering, National Fire Protection Association, Quincy (2002) 3.82–3.161. (Chapter 3–4).
[37] B. Schartel, M. Bartholmai, U. Knoll, Some comments on the use of cone calorimeter data, Polymer Degradation and Stability 88 (2005) 540–547.
[38] S.I. Stoliarov, S. Crowley, R.N. Walters, R.E. Lyon, Prediction of the burning rates of charring polymers, Combustion and Flame 157 (2010) 2024–2034.
[39] A.P. Mouritz, S. Feih, E. Kandare, Z. Mathys, A.G. Gibson, P.E. Des Jardin, et al., Review of fire structural modelling of polymer composites, Composites Part A Applied Science and Manufacturing 40 (2009) 1800–1814.
[40] W.D. Walton, P.H. Thomas, Estimating temperatures in compartment fires, SFPE Handbook of Fire Protection Engineering, National Fire Protection Association, Quincy (2002) 3.171–3.188. (Chapter 3–6).
[41] T.R. Hull, K. Lebek, M. Pezzani, S. Messa, Comparison of toxic product yields of burning cables in bench and large-scale experiments, Fire Safety Journal 43 (2008) 140–150.
[42] R. Kramer, P. Blomqvist, SP Report 2007:75 Fire Behaviour of Plastics for Electrical Applications, SP Technical Research Institute of Sweden, 2007.
[43] Panagiotou J., Quintiere J.G., Fire performance as a function of incident heat flux, in: The Fifth Triennial International Fire & Cabin Safety Research Conference, 2007, pp. 1–11.
[44] M.J. Scudamore, P.J. Briggs, F.H. Prager, Cone calorimetry—a review of tests carried out on plastics for the association of plastic manufacturers in Europe, Fire and Materials 15 (1991) 65–84.
[45] Mulholland G., Twilley W., Babrauskas V., Janssens M., Yusa S., The effect of oxygen concentration on CO and smoke produced by flames, in: The Third International Association for Fire Safety Science, 1991, pp. 585–594.
[46] L. Shi, M.Y.L. Chew, Q.Y. Xie, R.F. Zhang, L.M. Li, C.M. Xu, Experimental study on fire characteristics of PC monitors—Part II: Full-scale study under different ventilation conditions, Journal of Applied Fire Science 19 (2010) 41–61.
[47] W.K. Chow, S.S. Han, Studies on fire behaviour of video compact disc (VCD) materials with a cone calorimeter, Polymer Testing 23 (2004) 685–694.
[48] L. Shi, M.Y.L. Chew, A model to predict carbon monoxide of woods under external heat flux – Part II: Validation and application, Procedia Engineering – Proceedings of Ninth Asia-Oceania Symposium on Fire Science & Technology (2013). (In press).